#### ATOMS, MOLECULES, OPTICS =

## LASER COOLING OF YTTERBIUM-171 ION WITHOUT MAGNETIC FIELD

© 2024 O. N. Prudnikov \*\*, D. S. Krysenko \*\*, A. V. Taichenachev \*\*, V. I. Yudin \*\*, S. V. Chepurov \*\*, N. S. Lapin \*\*, and S. N. Bagaev \*\*, C. I. Yudin \*\*, J. Chepurov \*\*, N. S. Lapin \*\*, and S. N. Bagaev \*\*, C. I. Yudin \*\*, J. Chepurov \*\*, N. S. Lapin \*\*, and S. N. Bagaev \*\*, C. I. Yudin \*\*, J. Chepurov \*\*, N. S. Lapin \*\*, and S. N. Bagaev \*\*, C. I. Yudin \*\*, J. Chepurov \*\*, N. S. Lapin \*\*, J. Chepurov \*\*, J.

<sup>a</sup> Institute of Laser Physics, Siberian Branch of the Russian Academy of Sciences, Novosibirsk, 630090 Russia
 <sup>b</sup> Novosibirsk State Technical University, Novosibirsk, 630073 Russia
 <sup>c</sup> Novosibirsk State University, Novosibirsk, 630090 Russia

\*e-mail: oleg.nsu@gmail.com

Received April 27, 2024 Revised May 15, 2024 Accepted May 15, 2024

**Abstract.** A scheme for laser cooling of an  $^{171}{\rm Yb}^+$  ion in a radio-frequency trap using a three-frequency laser field with its components resonant to optical transitions of the line  $^2S_{1/2} \rightarrow ^2P_{1/2}$ , which does not require a magnetic field, is experimentally implemented. The exclusion of the magnetic field in the laser cooling cycle allows for precise control of a weak magnetic field ( $\sim 10^{-2}$  Gs), used for spectroscopy of clock transitions in the optical frequency standard based on a single ytterbium ion, which is important for suppressing frequency shifts associated with the quadratic Zeeman effect.

The article is presented as part of the conference proceedings "Physics of Ultracold Atoms" (PUCA-2023), Novosibirsk, December 2023.

**DOI:** 10.31857/S004445102410e122

#### 1. INTRODUCTION

Laser cooling of neutral atoms and ions is an important and integral stage in modern experiments in the field of quantum computing and simulations [1], as well as in creating modern frequency standards based on both cold neutral atoms in optical lattices [2–4] and ions in radio-frequency traps [5–7]. The achieved level of precision in optical frequency standards  $\Delta v / v < 10^{-18}$  opens up new horizons for the development of fundamental research such as studying the influence of Earth's gravitational field on the space-time continuum [3, 4, 8, 9], tests of the constancy of fundamental constants [10, 11], tests of general relativity theory, Lorentz invariance of space [12, 13, 14], dark matter search [15, 16], etc.

To achieve record levels of measurement accuracy in modern frequency standards, it is necessary to account for and suppress systematic shifts of atomic levels of various origins. For example, for a frequency standard based on a single ion, <sup>171</sup>Yb<sup>+</sup>, further progress in increasing accuracy may be associated

with controlling and suppressing shifts caused by equilibrium thermal radiation, systematic shifts due to the residual magnetic field, and shifts related to the quadratic Doppler effect [6, 13]. The main difficulty in suppressing magnetic field-induced shifts is that the transition used for laser cooling  ${}^2S_{1/2} \rightarrow {}^2P_{1/2}$ is not closed, and to implement cooling, laser field with two frequency components is typically used [17–19] (see Fig. 1a). In such a scheme, the magnetic field in the range of 1–10 G is required to destroy dark states appearing at the level  ${}^2S_{1/2}(F=1)$  due to coherent population trapping (CPT) effect. This allows achieving laser cooling temperature of the ion around the Doppler limit  $k_B T_D \simeq \hbar \gamma / 3$ , which is determined by the natural linewidth  $\gamma$  of the optical transition  ${}^2S_{1/2} \to {}^2P_{1/2}$ . Note that when implementing clock transition interrogations of the quadrupole  ${}^2S_{1/2}(F=0) \to {}^2D_{3/2}(F=2)$  or octupole  ${}^2S_{1/2}(F=0) \to {}^2F_{7/2}(F=3)$  transitions, the magnetic field used for cooling must be switched. the magnetic field used for cooling must be switched off and controlled at the level of about 0.03 G [19–21]. Hysteresis effects when switching off the magnetic

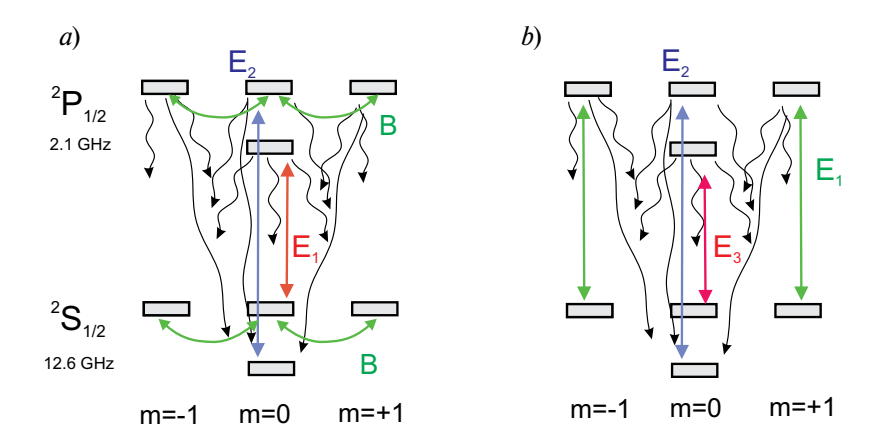


**Fig. 1.** Energy level scheme of hyperfine components of the states  ${}^2S_{1/2}$  and  ${}^2P_{1/2}$  used for laser cooling of ytterbium-171 ion in the presence of a magnetic field (a) and without magnetic field (b), according to the scheme proposed in [23]. Solid lines indicate forced resonant transitions caused by frequency components with co-directed linear polarizations. The magnetic field orthogonal to polarization vectors induces transitions between magnetic sublevels of states  ${}^2S_{1/2}(F=1)$  and  ${}^2P_{1/2}(F=1)$ 

field create significant difficulties for minimizing the residual magnetic field and maintaining it constant both in direction and amplitude during different cooling-interrogation cycles of the quantum system. Transition frequency shifts caused by the residual magnetic field of about 0.03 G are of the order of  $\Delta v / v_0 \sim 4 \cdot 10^{-17}$ , and their relative uncertainty is  $u / v_0 \sim 10^{-18}$  [6, 11]. Similar tasks of magnetic field control in different interrogation cycles arise in implementation of quantum logic elements and quantum computations based on  $^{171}{\rm Yb}^+$  ion ensembles [22].

In this work, we experimentally present a laser cooling method that does not require using a magnetic field proposed and theoretically studied by us in [23] (see Fig. 1b). To implement the proposed method, in addition to the cooling field scheme specified in work [23], we also need to modify the optical pumping scheme of the state  ${}^2D_{3/2}$ , which returns the ion to the laser cooling cycle.

### 2. LASER COOLING OF AN ION IN A THREE-FREQUENCY FIELD

For laser cooling of ytterbium-171 ion on a quasi-cyclic transition  ${}^2S_{1/2} \rightarrow {}^2P_{1/2}$ , we will use a polychromatic field having three frequency components with wave vectors along the z axis z

$$E(t) = \operatorname{Re}\left\{ \sum_{n=1,2,3} E_n e^{ik_n z} e^{-i\omega_n t} \right\}, \tag{1}$$

where complex vector amplitudes  $E_n$  are determined by polarizations, phases, and intensities of the frequency components (n=1,2,3),  $k_n$  are the corresponding wave vectors. For the cooling scheme in Fig. 1b the polarizations of the frequency components are chosen to be linear collinear, and their relative phase and coherence do not have a fundamental effect on ion cooling [23]. The frequencies of the components  $\omega_n$  are selected near the resonances of the corresponding transitions in Fig. 1b. Since the ion localization region l is small,  $l \ll \pi/|k_m - k_n|$  (for  $m \ne n$ ), the difference in phase accumulation of frequency components in the ion localization region can be neglected, setting all  $k_n$  equaling  $k_n = k = 2\pi/\lambda$  ( $\lambda = 370$  nm).

The problem of laser cooling of an ion in a radiofrequency trap can be solved within the quasiclassical approach using the Fokker-Planck equation for the distribution function in phase space F(z, p, t)

$$\left(\frac{\partial}{\partial t} + \frac{p}{M}\frac{\partial}{\partial z}\right)F = -\frac{\partial}{\partial p}F(z, p)F + \frac{\partial^2}{\partial p^2}D(p)F.(2)$$

Here  $F = F^{(s)}(v) + F^{(t)}(z)$  is the force at the point z acting on an ion moving with the velocity v and is the sum of spontaneous light pressure forces  $F^{(s)}(v)$  and contribution from the effective trap potential  $F^{(t)}(z) = -\nabla U_{osc}$ . The diffusion coefficient D(p) is determined by fluctuations of the particle momentum p = vM due to absorption and emission of field photons. Expressions for force and diffusion can be obtained directly during the reduction procedure of the quantum kinetic equation for the atomic density matrix to Fokker-Planck equation (2) [23, 24].

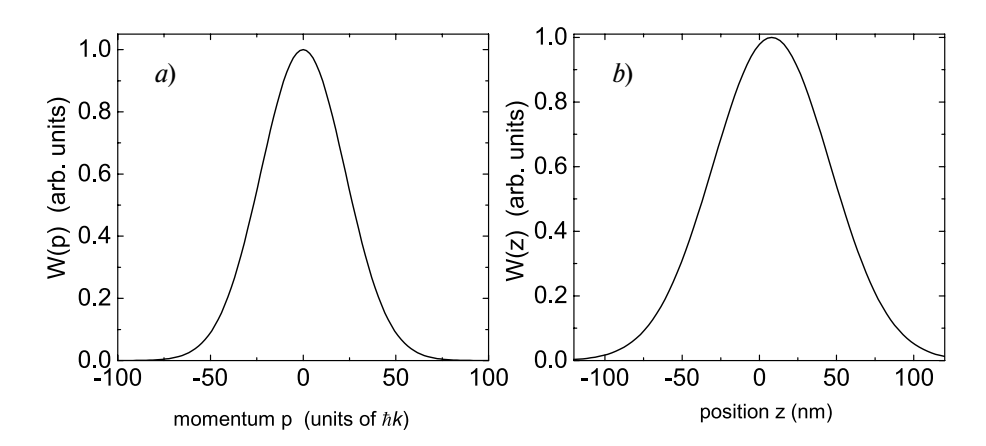
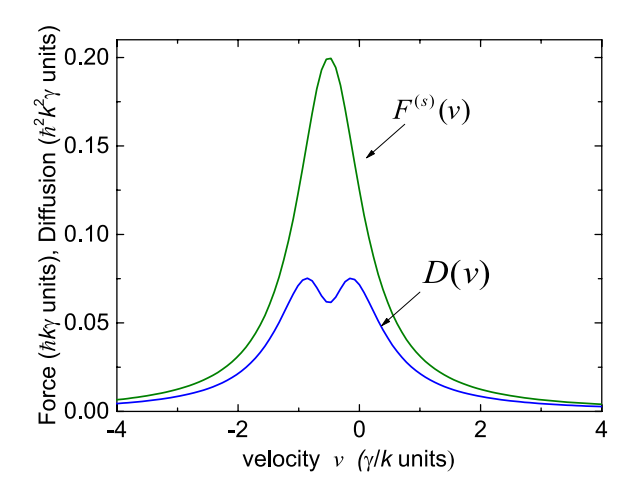


Fig. 2. Momentum W(z) and spatial W(p) distributions of the ion in the trap obtained through numerical solution of Fokker-Planck equation (2). Light field parameters correspond to Fig. 1. Ion oscillation frequency in the trap is  $\omega_{asc} = 600 \text{ kHz}$ 



**Fig. 3.** Dependence of the light pressure force  $F^{(s)}(v)$  and the diffusion coefficient D(v) on the ion velocity. The field is formed by waves with co-directed linear polarizations, Rabi frequencies of the fields  $\Omega_1 = \Omega_2 = \Omega_3 = \gamma$  correspond to the intensities of the frequency components I = 120 mW/cm², detunings  $\delta_1 = \delta_2 = \delta_3 = -\gamma/2$ 

The solution of Fokker-Planck equation (2) can be obtained numerically. In weak fields, when saturation parameters

$$S_n = \frac{|\Omega_n|^2}{\delta_n^2 + \gamma^2 / 4} \ll 1,$$

the expression for the temperature of cold atoms can also be obtained analytically [23]. Figure 2 shows the numerical steady-state solution of Fokker-Planck equation (2). For the parameters of Fig. 3, the momentum distribution of the ion in the trap

$$W(p) = \int F(z, p) dz$$

has the form of a Gaussian distribution with the temperature  $T \simeq 0.4\hbar\gamma$  /  $K_B$  (440 mK). Note that the spatial distribution of the ion

$$W(z) = \int F(z, p) dp$$

is shifted from the trap center by a value less than the size of the ion localization region, which is explained by the action of spontaneous light pressure force from the traveling components of light waves.

# 3. OPTICAL PUMPING OF STATE $^2D_{3/2}$ BY TWO INDEPENDENT LASERS WITH ORTHOGONAL POLARIZATIONS

The transition  ${}^2S_{1/2} \rightarrow {}^2P_{1/2}$  used for laser cooling of the ytterbium ion is not closed as there exists a radiative decay channel from the excited state  ${}^2P_{1/2}$  to the metastable state  ${}^2D_{3/2}$  with a rate of 90 kHz, see Fig. 4 To return the ion to the laser cooling cycle, typically (see, for example, [18, 19]) a two-frequency linearly polarized laser radiation is used, where one component is resonant with the transition  $F_D = 1 \rightarrow F_{[3/2]} = 0$ , and the other with the transition  $F_D = 2 \rightarrow F_{[3/2]} = 1$ , where  $F_D$  and  $F_{[3/2]}$ — are the total angular moments of hyperfine components of the states  ${}^2D_{3/2}$  and  ${}^3[3/2]_{1/2}$  respectively. In this case, dark states associated with coherent population trapping (CPT) effect on hyperfine sublevels  $F_D = 1$  and  $F_D = 2$  are destroyed by a sufficiently strong magnetic field oriented at a certain (optimal) angle relative to the polarization vector of the laser field. In our new laser cooling scheme, the magnetic field is absent, which requires using an optical pumping method different from

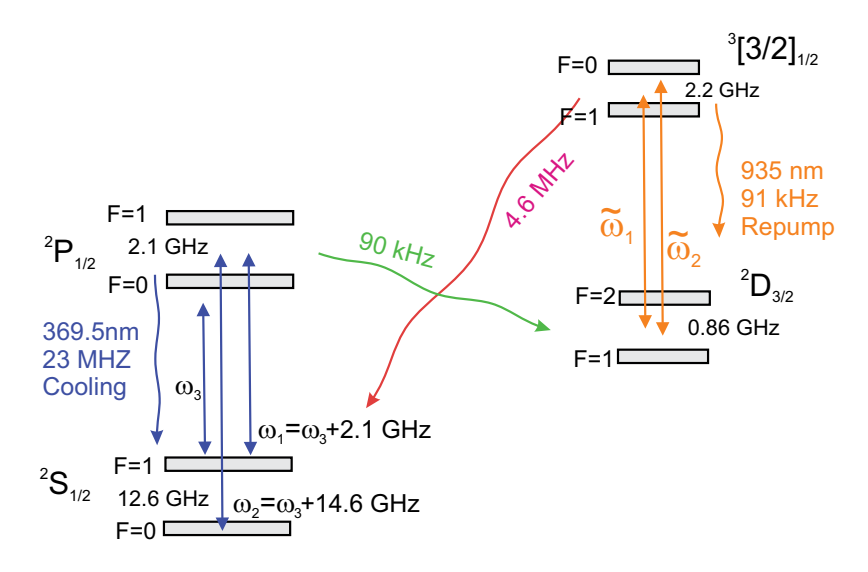


**Fig. 4.** Energy level diagram of ytterbium-171 ion. Arrows indicate forced transitions induced by the polychromatic field (369.5 nm) for laser cooling on the quasi-closed transition  ${}^2S_{1/2} \rightarrow {}^2P_{1/2}$ , as well as induced transitions of pump lasers (935 nm) for depopulation of the state  ${}^2D_{3/2}$ . Wavy lines indicate spontaneous decay channels with specified widths. Estimates of widths of decay channels  ${}^3[3/2]_{1/2} \rightarrow {}^2S_{1/2}^2$  and  ${}^2P_{1/2} \rightarrow {}^2D_{3/2}^2$  are based on data from [25]

the traditional one. Several different variants of effective optical pumping of state  $^2D_{3/2}$  in the zero magnetic field can be proposed using multifrequency laser radiation whose components have different polarizations. In this work, for technical reasons, we implement the simplest variant in some sense, based on using two independent lasers with orthogonal polarizations, whose frequencies are sufficiently detuned from transitions between hyperfine structure components of the states  $^2D_{3/2}$  and  $^3[3/2]_{1/2}$ . In this case, dark CPT states do not arise due to the combined independent action of radiation from two lasers. It is clear that the intensities of these radiations should be sufficiently high. However, the specific choice of frequencies and field intensities is not obvious in advance and requires physical and mathematical modeling.

Strictly speaking, the problems of laser cooling of ytterbium ion on the transition  ${}^2S_{1/2} \rightarrow {}^2P_{1/2}$  and optical pumping of the ion from the state  ${}^2D_{3/2}$  should be solved jointly based on the system of quantum kinetic equations for the ion density matrix, taking full account of the hyperfine and Zeeman structures of levels involved in radiative processes, as well as recoil effects during photon absorption and emission by the ion. Implementation of such a consistent program is possible but faces significant difficulties, mainly of technical nature. In this work, we use a simplified approach based on approximate separate consideration of these

two problems. In particular, if optical pumping of the state  ${}^2D_{3/2}$  works effectively, then the system of hyperfine and Zeeman sublevels of the transition  ${}^2S_{1/2} \rightarrow {}^2P_{1/2}$  can be approximately considered as closed and we arrive at the results of [23], which are briefly described above in Section 2. In turn, the system of hyperfine and Zeeman sublevels of the transition  ${}^2D_{3/2} \rightarrow {}^3 [3/2]_{1/2}$  is strongly open (see Fig. 4), and here the following approximate problem statement is possible. Initially, the ion is located on one of the sublevels of the state  ${}^{2}D_{3/2}$ (on any of them with equal probability). Then, under the action of fields exciting the transition  $^2D_{3/2} \rightarrow ^3[3/2]_{1/2}$  and due to spontaneous decay through the channel  $^3[3/2]_{1/2} \rightarrow ^2S_{1/2}$  the ion returns to the laser cooling cycle at the quasi-cyclic transition  $^2S_{1/2} \rightarrow ^2P_{1/2}$ . The problem is to find the average pumping time of the ion from the state  $^2D_{3/2}$ and then determine the optimal frequencies and intensities of fields for this process that minimize the average pumping time. This can be done using the  $\tau$ -matrix method developed by us earlier [26, 27]. We briefly state the main equations of the method. We assume that the density matrix  $\sigma$  describing the ion distribution over hyperfine and Zeeman sublevels of transition  ${}^2D_{3/2} \rightarrow {}^3[3/2]_{1/2}$  satisfies the quantum kinetic equation

$$\frac{d}{dt}\hat{\sigma} = -\hat{L}\{\hat{\sigma}\},\tag{3}$$

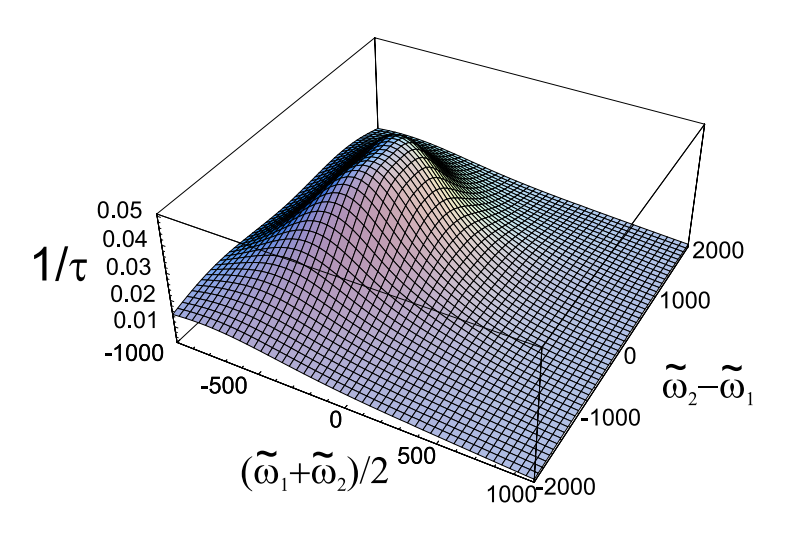


Fig. 5. Inverse pumping time  $1/\tau$  as a function of the difference  $\omega_2 - \omega_1$  and half-sum of frequencies  $(\omega_2 + \omega_1)/2$ . All values, including  $1/\tau$ , are given in MHz

where the Liouvillian  $\widehat{L}$  is a linear superoperator acting on the density matrix  $\widehat{\sigma}$  and describing light-induced and spontaneous transitions in the system of hyperfine and Zeeman sublevels of the transition  ${}^2D_{3/2} \rightarrow {}^3$  [3 / 2]<sub>1/2</sub>. The form of Liouvillian is given in the Appendix. Matrix  $\widehat{\tau}$  is defined as the time integral of the density matrix

$$\hat{\tau} = \int_{0}^{\infty} \hat{\sigma}(t) dt.$$

One can show that given the initial condition  $\hat{\sigma}(t=0) = \hat{\sigma}^{(0)}$  and final state  $\hat{\sigma}(t\to\infty) = 0$ , the elements of the matrix  $\hat{\tau}$  satisfy the system of linear algebraic equations

$$\widehat{L}\{\widehat{\tau}\} = \widehat{\sigma}^{(0)}. \tag{4}$$

The sought average pumping time  $\tau$  represents the sum of all diagonal elements of the matrix  $\tau$ 

$$\tau(I_1, I_2, \widetilde{\omega}_1, \widetilde{\omega}_2) = Tr\{\widehat{\tau}\}. \tag{5}$$

It depends on the problem parameters such as intensities  $I_i$  and frequencies  $\omega_i$  of laser fields. It can be shown that the pumping time defined this way has a lower limit min( $\tau$ ) = 2 /  $\gamma_{[3/2]}$ , where  $\gamma_{[3/2]}$  is the spontaneous decay rate of the state  $^3[3/2]_{1/2}$  to the ground state  $^2S_{1/2}$  (4.6 MHz).

With the given polarization values (linear, mutually orthogonal), intensities  $I_i$ , and frequencies

 $\omega_i$  of laser fields, the elements of the matrix  $\tau$  are found using the numerical solution procedure of system (4). We emphasize that for this choice of polarizations, this solution is unique. Ha fig. 5 shows the calculation results of the inverse pumping time  $\tau^{-1}$ , which represents the pumping rate at  $I_1 = I_2 = 150 \text{ W/cm}^2$  and varying frequencies  $\omega_i$  in sufficiently wide. In the case of equal field intensities, the pattern is symmetric with respect to the permutation of  $\omega_1 \leftrightarrow \omega_2$ . Therefore, it is convenient to switch to new variables, viz. the frequency difference  $\omega_2 - \omega_1$  and frequency halfsum  $(\omega_2 + \omega_1) / 2$ , which we will measure from the transition frequency  $F_D = 1 \rightarrow F_{[3/2]} = 1$ . The figure shows that there are two relatively smooth maxima located at the points  $(\omega_2 + \omega_1) / 2 \approx -350$  MHz and  $\omega_2 - \omega_1 \approx \pm 140$  MHz, where the pumping rate reaches values of  $1/\tau \approx 0.05$  MHz. This value is much lower than the theoretical limit of  $max(1/\tau) = \gamma_{[3/2]}/2 \approx 2$  MHz, but this level of optical pumping efficiency is sufficient for experimental implementation of laser cooling of vtterbium-171 ion in the zero magnetic field.

Time  $\tau$  in the experiment is typically not measured. However, this parameter affects the resonance fluorescence rate at the transition  ${}^2S_{1/2} \rightarrow {}^2P_{1/2}$ , which plays a key role in the ion laser cooling process and is directly measured in the experiment. To establish the correspondence between the resonance fluorescence rate and the optical pumping time, we will here (and only here) approximately consider the transition  ${}^2S_{1/2} \rightarrow {}^2P_{1/2}$ 

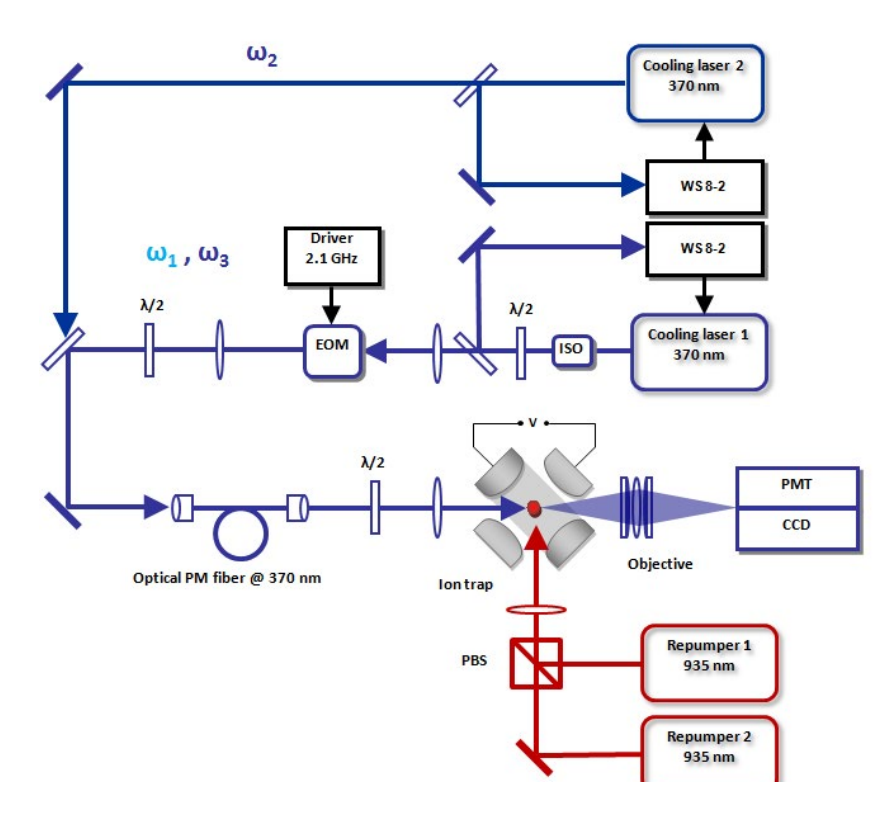


**Fig. 6.** Experimental setup scheme for ion cooling without magnetic field. EOM stand for the electro-optical modulator, ISO stand for the optical isolator, PMT stand for the photomultiplier tube, CCD stand for the CCD camera, and PBS stand for the polarizing beam splitter ranges

as a non-degenerate two-level system with an effective saturation parameter S. Then, we can show that the resonance fluorescence rate is determined by the expression

$$R = \frac{\gamma_{P}}{1 + (1 + S) / S + \gamma_{P \to D} \tau(I_{1}, I_{2}, \widetilde{\omega}_{1}, \widetilde{\omega}_{2})}, \quad (6)$$

where  $\gamma_P$  is the spontaneous decay rate through the channel  ${}^2P_{1/2} \rightarrow {}^2S_{1/2}$ ,  $\gamma_{P \rightarrow D}$  is the spontaneous decay rate through channel  ${}^2P_{1/2} \rightarrow {}^2D_{3/2}$ . A typical dependence of the rate R on the intensity of the pumping lasers (assuming  $I_1 = I_2 = I$ ) with optimal frequency selection  $((\omega_2 + \omega_1)/2 \approx -350 \text{ MHz}, \omega_2 - \omega_1 \approx \pm 140 \text{ MHz})$  and S = 1 is shown below in Fig. 7 in the experimentally accessible intensity range. This dependence qualitatively agrees with the experimental data (see below).

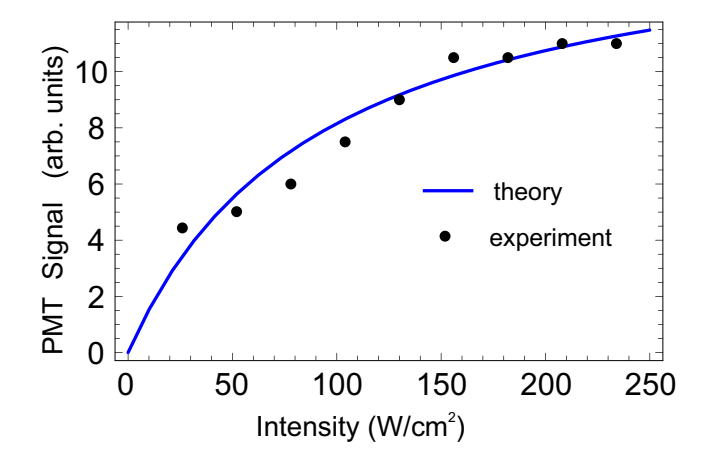
#### 4. EXPERIMENT

Figure 6 shows the scheme of the experimental setup implemented based on the optical frequency standard of a single ytterbium-171 ion developed at the Institute of Laser Physics SB RAS [28]

To capture and hold the ion, a miniature radio-frequency Paul trap with end electrodes is used [29]. This type of trap has an open design and, consequently, convenient ion loading and facilitated access for optical radiation. The trap electrodes, the ytterbium atom evaporation furnace, and three additional electrodes are used to apply DC voltage compensating for field asymmetry in the trap due to design imperfections or the presence of parasitic fields. To form a three-dimensional confining potential, an AC voltage with an amplitude of 600 V and frequency of 14 MHz is used. The potential well depth is 18 eV, with secular trap frequencies  $\omega_{osc,r} = 2\omega_{osc,r} = 1.2$ 

MHz. To increase ion holding time, the trap is placed in a vacuum chamber with the residual gas pressure less than  $5 \cdot 10^{-10}$  Torr, which helps minimize ion loss due to collisions with gas molecules.

Doppler cooling and ion detection are performed using polychromatic laser radiation on the quasicyclic transition  ${}^2S_{1/2} \rightarrow {}^2P_{1/2}$ . This scheme, as mentioned above, allows excluding the use of a



**Fig. 7.** Dependence of the fluorescence signal amplitude on the repumper intensity

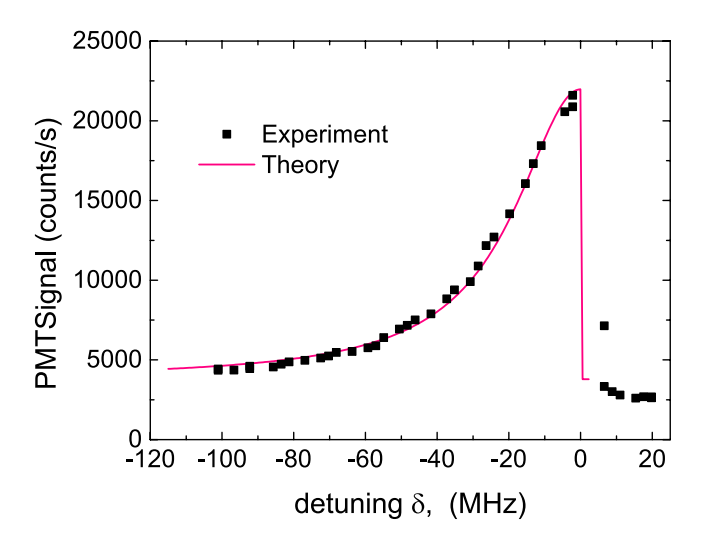


Fig. 8. Spectral profile of the fluorescence signal on the cooling transition of ytterbium-171 ion. The intensities of the cooling laser frequency components are equivalent and correspond to I=500 mW/cm² ( $\Omega\simeq2\gamma$ )

magnetic field for cooling and controlling it at a level below 0.03 G necessary for clock transition spectroscopy [19–21]. The cooling radiation was formed by combining beams from two semiconductor lasers, whose frequencies were stabilized using an Angstrom WS8-2 wavelength meter and were tuned to the components  $F = 1 \rightarrow F = 0$  (laser 1, frequency  $\omega_3$ ) and  $F = 0 \rightarrow F = 1$  (laser 2, frequency  $\omega_2$ ) of the cooling transition (Fig. 4). To generate the spectral component  $\omega_1$  exciting the cooling transition component  $F = 1 \rightarrow F = 1$ , laser 1 radiation is modulated by an electro-optical modulator (EOM) at a frequency of 2.1 GHz. The intensities of all fields are approximately the same,

with parallel linear polarizations and collinear beams.

The fluorescence radiation from the ion induced by the cooling laser is projected using a multi-lens objective onto a photomultiplier tube (PMT) and a charge-coupled device (CCD) matrix. The image on the CCD camera is used to determine the number of particles trapped in the trap, to monitor the ion's position in the trap, and for rough estimation of the ion temperature based on the cloud size. The PMT signal serves to determine the total fluorescence rate with high temporal resolution

To depopulate the levels  $^2D_{3/2}$  and  $^2F_{7/2}$  repumping diode lasers at wavelengths of 935 nm and 760 nm, respectively, are used. The repumping radiation at 935 nm was formed by combining beams from two frequency-unstabilized semiconductor lasers with linear orthogonal polarizations (Fig. 4).

In the proposed scheme of Doppler cooling without magnetic field, a fluorescence signal was obtained. The signal amplitude at the resonance center was about 20,000 photons/s, which is comparable to the traditional cooling scheme using a magnetic field and indicates comparable laser cooling efficiency. The maximum fluorescence signal is observed at repumper detuning of  $\widetilde{\omega}_2 - \widetilde{\omega}_1 \simeq 700 \pm 100$  MHz and intensities of each laser above 150 W/cm<sup>2</sup> (Fig. 7), which qualitatively corresponds to the theoretical analysis results from Section 3.

Figure 8 shows the resonant fluorescence signal on the cooling transition as a function of the total detuning  $\delta$  when choosing frequency component detunings equaling components equal to  $\delta_1 = \delta_2 = \delta_3 = \delta$ , and also at equal intensities of frequency components, i.e.,  $\Omega_1 = \Omega_2 = \Omega_3 = \Omega$ , which corresponds to the optimal laser cooling mode [23]. The theoretical fluorescence signal of the ion in the trap is represented as a convolution of excited state populations. The theoretical fluorescence signal of the ion in the trap is represented as a convolution of excited state populations  $\rho^e = \rho_1^e + \rho_0^e$  (where  $\rho_1^e$  and  $\rho_0^e$  are total populations of the states  $P_{1/2}(F=1)$  and  $P_{1/2}(F=0)$ , respectively) with the velocity distribution function of the cold ion W(v)

$$S(\delta,\Omega) = A \int \rho^{e}(\delta,\Omega,v)W(v)dv + B, \qquad (7)$$

where the coefficient A determines the signal detection efficiency, and B is the photodetector background signal.

The signal has a full width at half maximum (FWHM) of about 22 MHz, indicating that the ion is cooled and its motion does not contribute to the spectral line broadening. The drastic drop in the fluorescence signal for blue detuning is related to the fact that when the detuning sign changes, the laser cooling process turns into heating. An upper bound for the temperature can be obtained from the cloud size, which is smaller than the optical system resolution, yielding a value of about 100 mK.

#### 5. CONCLUSIONS

In this work, we experimentally implement an alternative laser cooling scheme <sup>171</sup>Yb<sup>+</sup> in a radiofrequency trap that does not require a magnetic field. The absence of the need for a magnetic field in the laser cooling cycle allows for precise control of the residual magnetic field, eliminating its fluctuations associated with switching on/off the magnetic field in the range of 1–10 G, which are required in standard ion laser cooling schemes.

Implementation of the presented ion laser cooling scheme also required modification of the optical pumping scheme needed for depopulation of the state  $^2D_{3/2}$ , to which decay from the state  $^2P_{1/2}$  is possible. The proposed optical pumping scheme using radiation from two independent lasers with orthogonal polarizations in the absence of a magnetic field demonstrated its effectiveness and allowed achieving fluorescence signal levels comparable to the standard scheme.

The presented scheme of laser ion cooling without using a magnetic field is promising for further increasing the accuracy of the optical frequency standard based on a single ion  $^{171}\mathrm{Yb^+}$ . Precise control of the residual magnetic field at a level below  $\sim 10^{-2}$  G will allow suppressing of magnetic field fluctuations and reducing the contribution to frequency uncertainty associated with the quadratic Zeeman effect to a level of u /  $v_0 \sim 10^{-19}$  and below.

#### **FUNDING**

The study was supported by the Russian Science Foundation, grant No. 23-22-00198, https://rscf.ru/project/23-22-00198/

#### APPENDIX.

#### QUANTUM KINETIC EQUATION FOR THE ION DENSITY MATRIX IN A TWO-FREQUENCY FIELD

We consider the quasi-resonant interaction of an ion in a system of hyperfine and Zeeman sublevels of transition  ${}^2D_{3/2} \rightarrow {}^3$  [3 / 2]<sub>1/2</sub> with a two-frequency field

$$\widetilde{E}(t) = \sum_{i=1,2} \widetilde{E}_i e_i e^{-i\widetilde{\omega}_i t} + \text{c.c.},$$
 (A.1)

where  $\widetilde{E}_i$  is the complex amplitude and  $e_i$  is the unit polarization vector i of the field component with frequency  $\widetilde{\omega}_i$ . The Hamiltonian of the ion in an external alternating field has the form

$$\widehat{H} = \widehat{H}_0 + \widehat{V}(t). \tag{A.2}$$

Here,  $\widehat{H}_0$  — is the Hamiltonian of a free ion, which we write as the sum of products of energies of hyperfine components of the states  ${}^2D_{3/2}$  and  ${}^3[3/2]_{1/2}$  on the corresponding projection operators

$$\widehat{H}_0 = \sum_{(F)} \left\{ E_{F_{[3/2]}} \widehat{\Pi}_{F_{[3/2]}} + E_{F_D} \widehat{\Pi}_{F_D} \right\}, \quad (A.3)$$

defined in the standard way through the sum of products of ket and bra vectors of Zeeman sublevels, for example

$$\widehat{\Pi}_{F_{D}} = \sum_{m=-F_{D}}^{F_{D}} |F_{D}, m\rangle\langle F_{D}, m|.$$

The operator of interaction with the laser field in the resonant and dipole approximations has the form

$$\widehat{V}(t) = \hbar \sum_{i=1}^{N} \Omega_{i} \widehat{D} \cdot e_{i} e^{-i\widetilde{\omega}_{i}t} + \text{H.c.}, \quad (A.4)$$

where Rabi frequencies are determined by the product of the reduced dipole moment of transition by the amplitude of the corresponding field component

$$\Omega_i = \frac{\tilde{d}\widetilde{E}_i}{\hbar},\tag{A.5}$$

and cyclic components of the dimensionless dipole moment operator are expressed through Clebsch-Gordan coefficients and 6 *j*-symbols as follows

$$\widehat{D} = \sum_{(F)} \widehat{D}(F_{[3/2]}, F_D);$$

$$\widehat{D}_q(F_{[3/2]}, F_D) \equiv \widehat{D}(F_{[3/2]}, F_D) \cdot e_q = (A.6)$$

$$= \sqrt{2(2F_D + 1)} \begin{cases} 3/2 & 1/2 & 1 \\ F_{[3/2]} & F_D & 1/2 \end{cases} \times \sum_{(\mu, m)} |F_{[3/2]}, \mu\rangle C_{F_D m 1 q}^{F_{[3/2]} \mu} \langle F_D, m|.$$

The quantum kinetic equation for the density matrix  $\sigma$  describing the distribution over internal degrees of freedom of the ion in the field (A.1) has the form

$$\frac{d}{dt}\widehat{\sigma} = -\frac{i}{\hbar} \left[ \widehat{H}_0, \widehat{\sigma} \right] - \frac{i}{\hbar} \left[ \widehat{V}(t), \widehat{\sigma} \right] - \widehat{\Gamma} \{\widehat{\sigma}\}. \quad (A.7)$$

Radiative relaxation is described by the operator  $\widehat{\Gamma}\{\widehat{\sigma}\}$ . All operators are represented by matrices in the basis of hyperfine and Zeeman sublevels of the transition  ${}^2D_{3/2} \rightarrow {}^3 [3/2]_{1/2}$  with the states  $\{|F_D,m\rangle\}$  and  $\{|F_{[3/2]},\mu\rangle\}$ . The density matrix  $\widehat{\sigma}$  can be divided into four matrix blocks, viz. the diagonal blocks  $\widehat{\sigma}_{DD}$  and  $\widehat{\sigma}_{[3/2][3/2]}$  can be considered as density matrices of corresponding levels, and the non-diagonal blocks  $\widehat{\sigma}_{[3/2]D}$  and  $\widehat{\sigma}_{D[3/2]}$  describe optical coherences between levels. We single out in the non-diagonal block rapid oscillations at the optical frequencies  $\widehat{\omega}_i$  explicitly  $\widehat{\sigma}_{[3/2]D}$ 

$$\hat{\sigma}_{[3/2]D} = \sum_{i=1}^{} \hat{\sigma}_{[3/2]D}^{(i)} e^{-i\tilde{\omega}_{i}t}.$$
 (A.8)

Matrices of relatively slowly varying amplitudes satisfy equations with constant coefficients

$$\left(\frac{d}{dt} + \frac{\gamma_{[3/2]}}{2} - i\widetilde{\omega}_i\right) \widehat{\sigma}_{[3/2]D}^{(i)} + \frac{i}{\hbar} \left[\widehat{H}_0, \widehat{\sigma}_{[3/2]D}^{(i)}\right] = 
= -i\Omega_i \left[\widehat{D} \cdot e_i \widehat{\sigma}_{DD} - \widehat{\sigma}_{[3/2][3/2]} \widehat{D} \cdot e_i\right]. \quad (A.9)$$

The quantum kinetic equations for diagonal blocks

$$\begin{split} &\left(\frac{d}{dt} + \gamma_{[3/2]}\right) \widehat{\sigma}_{[3/2][3/2]} + \frac{i}{\hbar} \left[\widehat{H}_0, \widehat{\sigma}_{[3/2][3/2]}\right] = \\ &= -i \sum_{i} \left[\Omega_i \widehat{D} \cdot e_i \widehat{\sigma}_{D[3/2]}^{(i)} - \widehat{\sigma}_{[3/2]D}^{(i)} \Omega_i^* (\widehat{D} \cdot e_i)^{\dagger}\right] - \end{split}$$

$$-i\sum_{i\neq j} \left[ \Omega_{i} \widehat{D} \cdot e_{i} e^{-i(\widetilde{\omega}_{i} - \widetilde{\omega}_{j})t} \widehat{\sigma}_{D[3/2]}^{(j)} - i\sum_{i\neq j} \left[ \Omega_{i} \widehat{D} \cdot e_{i} e^{-i(\widetilde{\omega}_{i} - \widetilde{\omega}_{j})t} \widehat{\sigma}_{D[3/2]}^{(j)} - \widehat{\sigma}_{D[3/2]D} \Omega_{i}^{*} (\widehat{D} \cdot e_{i})^{\dagger} e^{i(\widetilde{\omega}_{i} - \widetilde{\omega}_{j})t} \right]$$

$$- \alpha_{[3/2] \to D} \sum_{q=0,\pm 1} \widehat{D}_{q}^{\dagger} \widehat{\sigma}_{[3/2][3/2]} \widehat{D}_{q} = -i\sum_{i} \left[ \Omega_{i}^{*} (\widehat{D} \cdot e_{i})^{\dagger} \widehat{\sigma}_{[3/2]D}^{(i)} - \widehat{\sigma}_{D[3/2]D}^{(i)} \widehat{D} \cdot e_{i} \right] - -i\sum_{i\neq j} \left[ \Omega_{i}^{*} (\widehat{D} \cdot e_{i})^{\dagger} e^{i(\widetilde{\omega}_{i} - \widetilde{\omega}_{j})t} \widehat{\sigma}_{[3/2]D}^{(j)} - \widehat{\sigma}_{D[3/2]D}^{(j)} - \widehat{\sigma}_{D[3/2]D}^{(j)} \widehat{D}_{i} (\widehat{D} \cdot e_{i})^{\dagger} e^{i(\widetilde{\omega}_{i} - \widetilde{\omega}_{j})t} \widehat{\sigma}_{[3/2]D}^{(j)} - \widehat{\sigma}_{D[3/2]D}^{(j)} \widehat{D}_{i} (\widehat{D} \cdot e_{i}) e^{-i(\widetilde{\omega}_{i} - \widetilde{\omega}_{j})t} \right]$$

$$(A.11)$$

contain terms (last two lines in (10) and (11)) oscillating at the frequency difference  $\omega_2 - \omega_1$ . These terms describe the joint coherent action of frequency field components and lead to a number of important phenomena in nonlinear optics and spectroscopy related to quantum beats, in particular, to coherent population trapping resonances (see, for example, [30]). However, for the frequency range considered in this work  $\omega_i$ , which are sufficiently detuned (by hundreds of MHz) from both single-photon and two-photon resonances and field intensities (corresponding Rabi frequencies  $\Omega$ , do not exceed 200 MHz), the formation of higher harmonics of the density matrix  $\sigma$  at frequency differences occurs with low efficiency and practically does not affect the optical pumping process. For this reason, here we will limit ourselves to the zero approximation, omitting the second lines in equations (10) and (11), which corresponds to joint but completely independent action of two pumping lasers. Obviously, the system of equations (9)–(11) can be represented as a system of ordinary differential equations with constant coefficients (3). Thus, Eqs. (9), (10) define in the considered approximation the superoperator  $\hat{L}$ . As for the initial condition  $\hat{\sigma}^{(0)}$ , which appears in Eq. (4), it corresponds to a uniform and isotropic distribution over the sublevels of the state  ${}^2D_{3/2}$ 

$$\widehat{\sigma}^{(0)} = \frac{\sum_{F_D} \widehat{\Pi}_{F_D}}{8}.$$
 (A.12)

#### **REFERENCES**

- 1. M. A. Nielsen, and I.L. Chuang, *Quantum Computation and Quantum Information*, Cambridge University Press (2010).
- 2. S. Falke, N. Lemke, Ch. Grebing et al., New J. Phys. **16**, 073023 (2014).
- 3. M. Takamoto, I. Ushijima, N. Ohmae, T. Yahagi, K. Kokado, H. Shinkai, and H. Katori, Nat. Photonics 14, 411 (2020).
- W. F. McGrew, X. Zhang, R. J. Fasano, S. A. Schaffer, K. Beloy, D. Nicolodi, R. C. Brown, N. Hinkley, G. Milani, M. Schioppo, T. H. Yoon, and A. D. Ludlow, Nature 564, 87 (2018).
- 5. C. W. Chou, D. B. Hume, J. C. J. Koelemeij, D. J. Wineland, and T. Rosenband, Phys. Rev. Lett. **104**, 070802 (2010).
- **6.** N. Huntemann, C. Sanner, B. Lipphardt, C. Tamm, and E. Peik, Phys. Rev. Lett. **116**, 063001 (2016).
- Y. Huang, H. Guan, P. Liu, W. Bian, L. Ma, K. Liang, T. Li, and K. Gao, Phys. Rev. Lett. 116, 01300 (2016).
- **8**. G. Lion, I. Panet, P. Wolf, C. Guerlin, S. Bize, and P. Delva, J. Geodes. **91**, 597 (2017).
- 9. W. F. McGrew, X. Zhang X, R. J. Fasano, S. A. Schaffer, K. Beloy, D. Nicolodi, R. C. Brown, N. Hinkley, G. Milani, M. Schioppo, T.H. Yoon, and A. D. Ludlow, Nature **564**, 87 (2018).
- R. M. Godun, P. B. R. Nisbet-Jones, J. M. Jones, S. A. King, L. A. M. Johnson, H. S. Margolis, K. Szymaniec, S. N. Lea, K. Bongs, and P. Gill, Phys. Rev. Lett. 113, 210801 (2014).
- 11. N. Huntemann, B. Lipphardt, C. Tamm, V. Gerginov, S. Weyers, and E. Peik, Phys. Rev. Lett. 113, 210802 (2014).
- **12**. V. Dzuba, V. V. Flambaum, M. S. Safronova, S. G. Porsev, T. Pruttivarasin, M. A. Hohensee, and H. Haffner, Nature Physics **12**, 465 (2016).
- 13. C. Sanner, N. Huntemann, R. Lange, C. Tamm, E. Peik, M. S. Safronova and S. G. Porsev, Nature 567, 2048 (2019).
- **14.** L. S. Dreissen, C.-H. Yeh, H. A. Fürst, K. C. Grensemann, and T. E. Mehlstäubler, Nature Commun. **13**, 7314 (2022).

- **15**. A. Arvanitaki, J. Huang, and K.V. Tilburg, Phys. Rev. D **91**, 015015 (2015).
- **16**. Y.V. Stadnik, and V.V. Flambaum, Phys. Rev. Lett. **115**, 201301 (2015).
- **17**. Chr. Tamm, S. Weyers, B. Lipphardt, and E. Peik, Phys. Rev. A **80**, 043403 (2009).
- O. N. Prudnikov, S. V. Chepurov, A. A. Lugovoy, K. M. Rumynin, S. N. Kuznetsov, A. V. Taichenachev, V. I. Yudin, and S. N. Bagayev, Quant. Electron. 47, 806 (2017).
- **19**. S. V. Chepurov, A. A. Lugovoy, O. N. Prudnikov, A. V. Taichenachev, and S. N. Bagayev, Quant. Electron. **49**, 412 (2019).
- **20**. N. Huntemann, M. Okhapkin, B. Lipphardt, S. Weyers, Chr. Tamm, and E. Peik, Phys. Rev. Lett. **108**, 090801 (2012).
- **21.** N. Huntemann, B. Lipphardt, M. Okhapkin, Chr. Tamm, E. Peik, A. V. Taichenachev and V. I. Yudin, Phys. Rev. Lett. **109**, 213002 (2012).
- 22. M. A. Aksenov, I. V. Zalivako, I. A. Semerikov, A. S. Borisenko, N. V. Semenin, P. L. Sidorov, A. K. Fedorov, K. Yu. Khabarova, and N.N.Kolachevsky, Phys. Rev. A 107, 052612 (2023).
- **23**. D. S. Krysenko and O. N. Prudnikov, JETP **137**, 239 (2023).
- **24**. O. N. Prudnikov, A. V. Taichenachev, A. M. Tumaikin and V. I. Yudin, JETP **88**, 433 (1999).
- 25. E. Biemontyz, J-F Dutrieuxz, I. Martinx, and P. Quinetz, J. Phys. B: At. Mol. Opt. Phys. 31, 3321 (1998.)
- **26**. A. V. Taichenachev, A. M. Tumaikin, V. I. Yudin, and L. Hollberg, Phys. Rev. A **63**, 033402 (2001).
- A. P. Kulosa, O. N. Prudnikov, D. Vadlejch, H. A. Furst, A. A. Kirpichnikova, A. V. Taichenachev, V. I. Yudin, and T. E. Mehlstaubler, New J. Phys. 25 053008 (2023).
- **28.** S. V. Chepurov, N. A. Pavlov, A. A. Lugovoy, S. N. Bagayev, and A. V. Taichenachev, Quantum Electronics **51**, 473 (2021).
- **29**. C. A. Schrama, E. Peik, W. W. Smith, and H. Walther, Opt. Comm. **101**, 32 (1993).
- **30**. A. V. Taichenachev, V. I. Yudin, R. Wynands, M. Stahler, J. Kitching, and L. Hollberg, Phys. Rev. A **67**, 033810 (2003).